

Received October 21, 2019, accepted November 13, 2019, date of publication November 21, 2019, date of current version December 4, 2019.

Digital Object Identifier 10.1109/ACCESS.2019.2954863

# Smart Longitudinal Velocity Control of Autonomous Vehicles in Interactions With Distracted Human-Driven Vehicles

WEN YAN<sup>1</sup>, (Student Member, IEEE), CHUNGUO LI<sup>1</sup>, (Senior Member, IEEE),  
YONGMING HUANG<sup>1</sup>, (Senior Member, IEEE),  
AND LUXI YANG<sup>1</sup>, (Senior Member, IEEE)

School of Information Science and Engineering, Southeast University, Nanjing 210096, China

Corresponding author: Luxi Yang (lxyang@seu.edu.cn)

This work was supported in part by the National Natural Science Foundation of China under Grant 61971128 and Grant 61671144, and in part by the National Key Research and Development Program of China under Grant 2018YFB1800801.

**ABSTRACT** With the development of commercialized autonomous vehicles (AVs), the interaction between AVs and human-driven vehicles has become increasingly important. Nevertheless, on the one hand, complex driver behaviors like distraction are hard to detect by AVs, which may lead to traffic accidents because of the late alert to the following vehicles. On the other hand, advanced techniques such as the real-time image or video processing and vehicle-to-vehicle (V2V) communications make it possible to let AVs receive monitoring signals from nearby vehicles, predict the latent risks, and make smart control to avoid the vehicles driven by distracted drivers. Hence, in this paper, we envisage a collaborative framework integrating human driver distraction monitoring, V2V communications, and AV velocity control. Then, we design the smart velocity control of AVs by taking into consideration the distraction behaviors of the drivers in the human-driven vehicles, and by formulating it as a feasible optimization problem based on model predictive control (MPC) strategies. Furthermore, we analyze the safety benefits that the collaborative framework could help improve on the condition of preserving traffic performance. Finally, we implement the contrast tests of real-time evaluation on driver distraction monitoring based on convolutional neural networks (CNNs) and perform simulations of smart velocity control strategies of the AV at avoiding the distracted driver and reducing rear-end collisions. Through the analysis and the simulations, we show our framework could increase the safety regions, reduce the rear-end collisions, and thus increase the safety of the whole transportation networks.

**INDEX TERMS** Autonomous vehicle, distraction monitoring, velocity control, model predictive control, convolutional neural networks.

## I. INTRODUCTION

In recent years, intelligent transportation system (ITS) has attracted much attention from both academia and industry, which is expected to improve transportation safety and mobility [1]–[3]. As one of the significant technologies, autonomous driving systems have been aimed to bring us safety, as well as autonomy, namely making driving decisions independently [4]–[6]. Meanwhile, much attention has been paid to the theoretical research and industrial practice of autonomous vehicles (AVs) [7]–[9].

The associate editor coordinating the review of this manuscript and approving it for publication was Yang Tang<sup>1</sup>.

Nevertheless, AVs and human drivers are expected to coexist for a long time. Thus, it is important to consider their interactions [10], [11]. In particular, on the one hand, the driving manner of AVs may seem to be stubborn without face-to-face communications between human drivers. For instance, many AVs only use on-board sensors to perceive the environment thus having difficulties anticipating the motion of surrounding human-driven vehicles [12]. On the other hand, the implicit and complex states and behaviors of human drivers like distractions and fatigue, which are hard to detect by the AVs, may result in sudden brakes and subsequent accidents because of the late alert to the following AVs. Moreover, the movements of human-driven vehicles usually

involve a high level of uncertainty and randomness [13], and sometimes human drivers dangerously trade off safety for throughput [14], both bringing potential risks to the AVs. Current research on AV control mainly focuses on the operations like car-following [15], lane-changing [16], or assisted driving for the drivers inside vehicles [17], and it often ignores the interactions between AVs and human-driven vehicles. Even there exists some related work, it mainly resides in sharing roads and the passing policy at the road intersections [18], [19], or simply sending out alerts in the case of emergency [20]. Recently, there also appears some pioneering studies like improving the throughput by a cooperative platoon control of mixed AVs and human-driven vehicles [13], [14] or mitigating the cascade of braking events by using the motion information of nearby human-driven vehicles for the AV [12]. However, in a nutshell, current studies in AV control have not fully exploited complex driver behaviors like distractions to make smart control.

However, there is no doubt that driver distraction has become a crux safety concern in transportation networks. It is regarded as one main form of inattention which is involved in at least 25% of police-reported crashes as reported by the National Highway Traffic Safety Administration [21]. What's more, it is found that almost 80% of all crashes and 65% of all near-crashes involve driver distractions [22]. As a result, it's meaningful to take the complex distraction behaviors of human drivers into consideration, which can guide AVs to perform smart control decisions independently and avoid abnormal drivers carefully like experienced drivers, not only execute the processes and procedures without human interventions as required by automated vehicles [23], [24]. Nevertheless, the appealing idea brings several difficulties as well: (1) the implicit distraction behaviors need to be detected and processed in an acceptable delay on the side of human drivers; (2) the information on driver distraction behaviors should be effectively evaluated and incorporated into the AV control once being obtained by the AV; and (3) a collaborative framework needs to be designed to support the whole procedures spanning computer vision, communication and control areas from both the human driver side and the AV side.

As for the related work on AV control and autonomous driving systems, the role of vehicle control is to enhance the robustness and stability of the system in the presence of modeling error and uncertainties [25]. Typical control design methods include static feedback control, optimal control, MPC, and artificial intelligence techniques [26]. Static feedback control methods determine control actions based on the current state of the system, but they cannot handle any external constraints [27]. Optimal control and MPC are two dynamic control methods which use optimization algorithms to determine optimal control actions based on real-time measurements. Optimal control suffers from the disturbances and model mismatch errors because of its intrinsic open-loop control approach [28]; MPC uses a rolling horizon approach that introduces a feedback mechanism, which

can make the controlled system more robust to uncertainties and disturbances than optimal control [29]. In practice, MPC-based methods have been widely demonstrated in real-time applications in AVs [25], [30], [31]. What's more, artificial intelligence techniques including case-based reasoning, fuzzy logic, rule-based system, etc., are always used when explicit models are not available, which we refer the readers to [26] for more details. Recently, there have already been some pioneering studies to introduce the role of human drivers into the guidance of AVs. Lefèvre *et al.* [30] present a framework for autonomous driving which can learn from human demonstrations, and apply the demonstrations to the longitudinal control of an autonomous car. Tehrani *et al.* [32] compare the actions of a human driver with computer generated motions for expressway lane changing. By analyzing the human-driver lane change data, Do *et al.* [33] propose a two-segment lane change model that mimics the human driver. Nevertheless, most of these studies focus on imitating human drivers in the AV control, while none of them consider the active management of AVs with distracted drivers.

The work presented in this paper is to build a bridge between the AV control and the driver behavior detection by focusing on the longitudinal velocity control of AV to avoid potential distracted human drivers. To concentrate on establishing a whole mechanism to support the AV to predict the latent risks and actively avoid abnormal drivers, in the rest of the paper, we consider the basic car-following scenario, namely that an AV follows a human-driven vehicle. We aim to establish a framework to make AV drive smarter to adaptively spare more relative distances when the preceding driver falls into distraction. The main insight of the proposed framework is that the distracted human driver will decrease his/her driving ability and may make strong brakes to deal with a sudden emergency, thus leading to potential rear-end collisions for the following "unaware" vehicles. In more details, on the one hand, it's hard for the AV to avoid the distracted human driver since the distraction state of the driver cannot be detected by the AV. Furthermore, even the AV can take advantage of its short responding time to avoid the collision, it's much harder for its followers especially human drivers to stop in time because of the late alert. Therefore, we want to make an attempt to address how the AV could make longitudinal velocity control to avoid distracted human drivers in this paper. By jointly dealing with the above-discussed challenges, our main technical contributions can be summarized as follows:

- *Collaborative Framework*: To make AV aware of the potential risks, we need collaborations from multiple areas. Thus we put forward a practical system framework integrating driver distraction monitoring, V2V communications, and AV velocity control.
- *Smart Longitudinal Velocity Control of AV to Avoid Distracted Driver*: The detected driver distraction information cannot be directly used to guide the AV, thus we evaluate the influence of driver distraction behaviors from two aspects: the risk and the confidence, and integrate them into longitudinal velocity control of AV.

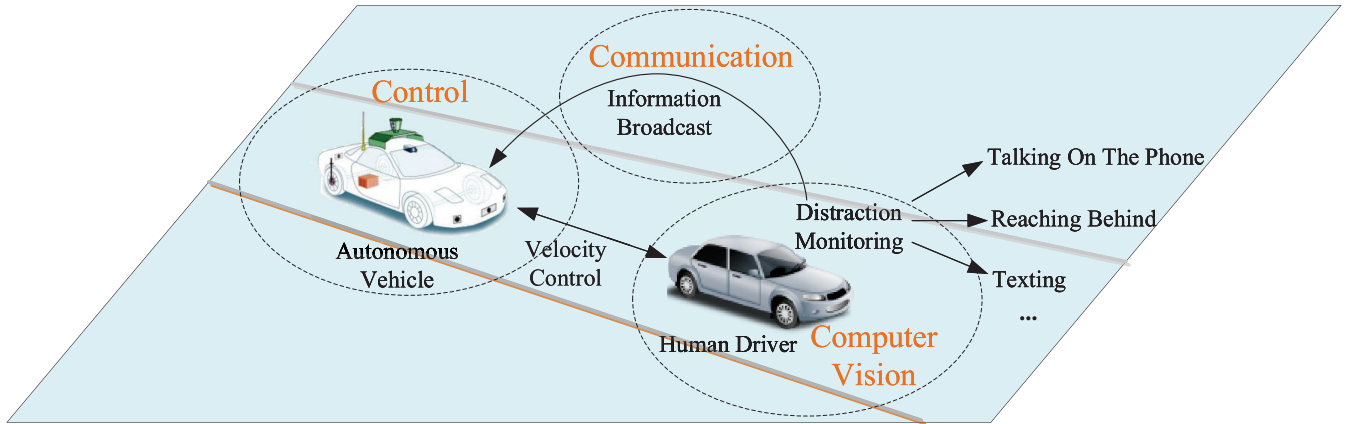


FIGURE 1. Illustration of the collaborative framework.

Then, we formulate it as a feasible optimization problem based on model predictive control (MPC) strategies.

- *Benefit Analysis of the Framework:* We analyze and visualize the safety benefits by comparing the increase of safety regions with and without the system framework on the condition of preserving the traffic performance.
- *Simulations:* We perform two simulations to validate the effectiveness of our system framework and control strategies: driver distraction monitoring based on the convolutional neural networks (CNNs) model and longitudinal velocity control of AV .

The rest of this paper is organized as follows. Section II proposes a collaborative framework. Section III puts forward an MPC-based optimization method of longitudinal velocity control of AV by taking driver distractions into consideration. Section IV analyzes the safety benefits the collaborative framework could help improve. The simulation results are provided in Section V. Finally, we conclude the whole paper in Section VI and several technical details are deferred to the appendices.

*Notation:* Uppercase letters denote matrixes and bold lowercase letters refer to column vectors. Operators  $(\cdot)^T$  and  $\text{tr}(\cdot)$  indicate transposition and matrix trace, respectively.  $\mathbb{R}$  represents the real number set, and  $\mathbb{R}_+$  is its positive part.  $\mathbb{N}_+$  denotes the positive integer set.  $\log(x)$  returns the natural logarithm of  $x$ . A  $K$ -dimensional column vector of all ones is presented by  $\mathbf{1}_K$ .  $|\cdot|$  represents the absolute value of a scalar.  $\|\cdot\|_2$  presents the 2-norm of a vector. The Frobenius norm of matrix  $A = [a_{i,j}] \in R^{m \times n}$  is  $\|A\|_F := \sqrt{\text{tr}(AA^T)}$ .  $\cos(x)$  is the cosine of  $x$ .  $\text{angle}(\mathbf{a}, \mathbf{b})$  denotes the angle between vector  $\mathbf{a}$  and vector  $\mathbf{b}$ .

## II. COLLABORATIVE FRAMEWORK

In this section, we put forward a practical collaborative framework integrating driver distraction monitoring, V2V communications, and AV velocity control, which spans computer vision, communication and control areas.

As shown in Fig.1, the collaborative framework consists of three parts: real-time distraction monitoring on the side of the human driver, information transmission to AV through V2V communications, and longitudinal velocity control on the AV side. Here, we consider the car following scenario and without loss of generality assume the AV follows a human-driven car on the same lane.

The part of real-time distraction monitoring could be performed by computer vision techniques, such as popular convolutional neural networks (CNNs), based on real-time sensed images or video streams. With the popularization of assisting driving systems, this part can be easily implemented by cameras and processors in the driver’s car or just an active monitoring application installed in the smart mobile phone [34]. Due to the privacy concern, the results should be sensed under the authorization of the driver and encrypted before transmission using the encryption techniques like simple interleaving or differential privacy [35] and so on. What’s more, based on the distraction monitoring results, the human-driven vehicle could send alerts to the distracted driver and send the encrypted results to the following AV to let the AV drive more cautiously, both for the safety concern of the human driver. Thus, it would become easier for the human driver to accept the distraction monitoring. Moreover, considering the distraction usually lasts for a while, the detection based on the anomalies of the vehicle dynamic movement may not work in time compared to the real-time distraction monitoring based on computer vision techniques, since the anomalies commonly not appear at the very beginning stage of the distraction of the human driver.

Information broadcast through V2V communications is aimed to be supported by the communicators equipped within both vehicles and the techniques like millimeter wave technologies [36]–[38]. To be practical and efficient, we assume only the encrypted vector of classification probability is transferred.

The part of longitudinal velocity control at the AV side is based on model predictive control (MPC) strategies, which

applies optimization algorithms to determine optimal control actions based on real-time measurements.

Next, we focus our attention on designing the smart longitudinal velocity control of AV.

### III. SMART LONGITUDINAL VELOCITY CONTROL OF AV TO AVOID DISTRACTED DRIVER

In this section, we propose the adaptive longitudinal velocity control of AV according to the human driver's distraction behaviors. We firstly introduce the vehicle model. Then we evaluate the risk caused by driver distraction behaviors and the confidence of the received monitoring result. Next, safety constraints are given with persistent feasibility analyzed. Finally, we integrate the risk and the confidence to design the cost function and adopt MPC strategies to formulate the longitudinal velocity control into a feasible optimization problem.

#### A. VEHICLE MODEL

To depict the longitudinal velocity control of AV, we use  $\xi_t = [d_t, v_t]^T$  to present the state of the AV at time  $t \in \mathcal{T}$ , where  $\mathcal{T}$  denotes the unique time set of the system, and  $d_t \in \mathbb{R}_+$  and  $v_t \in \mathbb{R}_+$  are the longitudinal position of the AV in a road-aligned coordinate system and its longitudinal velocity, respectively, and likewise for  $\xi_t^p = [d_t^p, v_t^p]^T$  of the vehicle driven by the human.

The acceleration sequence is denoted as  $\mathbf{a}_t = [a_t, \dots, a_{t+N_c-1}]^T$  with  $a_t \in \mathbb{R}$ ,  $t \in \mathcal{T}$ , and  $N_c = T_c/\Delta t_c$  is the number of time steps in the prediction horizon  $T_c \subset \mathcal{T}$  for the controller's sampling time  $\Delta t_c$ . Here acceleration sequence  $\mathbf{a}_t$  is the optimization variable we focused on in the longitudinal velocity control of the AV.

For demonstration, we adopt a kinematic point-mass model for the AV [30], since the longitudinal motions could reduce the degree of freedom of vehicle model from six to one [39]. The state update equations are given by

$$d_{k+1|t} = d_{k|t} + v_{k|t}\Delta t_c + \frac{1}{2}a_{k|t} \cdot (\Delta t_c)^2 \quad (1a)$$

$$v_{k+1|t} = v_{k|t} + a_{k|t} \cdot \Delta t_c \quad (1b)$$

where the variable  $v_{k|t}$  for  $k \in \mathbb{N}_+$  denotes the predicted value of  $v$  at time  $t+k \in \mathcal{T}$  based on information available at time  $t$ , and denotes the history value of  $v$  at time  $t+k \in \mathcal{T}$  for  $k \leq 0$ , same for other variables. Compactly, the linear time-invariant vehicle model is written in a state-space form with  $C$  and  $D$  denoting the state matrixes as:

$$\xi_{k+1|t} = C\xi_{k|t} + Da_{k|t}, \quad (2)$$

where  $C$  and  $D$  only depend on  $\Delta t_c$ , the controller's sampling time of AV.

Similarly, we assume the human-driven vehicle fit the kinematic point-mass model. What's more, from the AV control system perspective, we assume  $\Delta t_c$  could characterize the predicted motions of the human-driven vehicle thus same  $C$

and  $D$  could be adopted. The state update equations of the human-driven vehicle are as follows:

$$\xi_{k+1|t}^p = C\xi_{k|t}^p + Da_{k|t}^p \quad (3)$$

where  $a_t^p$  denotes the acceleration at time  $t$  of the human-driven vehicle.

Since the AV cannot obtain the future actions of the vehicle driven by the human, here for the consideration of robustness, we treat  $a_t^p$  as a disturbance in our analysis, and formulate its value range as follows:

$$a_t^p \in \mathcal{A}^p := \{x : a_{\min}^p \leq x \leq a_{\max}^p\} \quad (4)$$

where  $a_{\min}^p$  and  $a_{\max}^p$  are the estimated acceleration bounds of the human-driven vehicle.

#### B. RISK EVALUATION

In order to characterize different distraction behaviors more meticulously thus letting the AV deal with various distraction scenarios properly, in this subsection, we first define the risk caused by driver distraction behaviors, followed by the heuristic definition of the penalty for different distraction behaviors from a probability perspective.

To facilitate the subsequent analysis, we assume at the driver side the distraction monitor generates a sequence of monitoring results  $\{c_t \in \mathbb{R}_+^K | c_t^T \cdot \mathbf{1}_K = 1, t \in \mathcal{T}\}$  with time interval  $\Delta t_d$ , where the equation property results from the probabilistic output of the distraction behavior classifier and  $K$  is the number of classes. (For example, in the subsequent simulation part, we use CNN to get the monitoring results and consider the distraction behaviors listed in Table 1, and the readers could get more details in Section V.A.) Then the human-driven vehicle sends the probably encrypted monitoring results to the following AV through V2V communications shown in Fig. 1. Next, we assume on the AV side, the AV receives and decrypts the sequence of monitoring results and gets  $\{\hat{c}_t\}_{t \in \mathcal{T}}$ . For simplicity, we assume that we still have  $\hat{c}_t \in \mathbb{R}_+^K$  with time interval  $\Delta t_d$ , but  $\hat{c}_t^T \cdot \mathbf{1}_K = 1$  may not hold any more due to the noises resulting from V2V communications, leading to the confidence evaluation in the next subsection.

To account for the risk, on the AV side, after receiving the monitoring result  $\hat{c}_t$  at time  $t \in \mathcal{T}$ , the risk  $r_t$  can be evaluated by using a penalty vector  $\mathbf{h}$  which characterizes the penalties of different distraction behaviors as follows:

*Definition 1:* Consider the car-following scenario as shown in Fig.1, the risk  $r_t$  to the AV caused by the distraction result  $\hat{c}_t$  from the preceding human driver at time  $t \in \mathcal{T}$  can be evaluated as:

$$r_t := r_{\text{norm}} \hat{c}_t^T \cdot \mathbf{h}, \quad t \in \mathcal{T} \quad (5)$$

where  $r_{\text{norm}}$  is the tuning parameter which can normalize the value of  $r_t$ .

Notice that under this definition, a bigger value of  $r_t$  indicates a higher potential risk suffered by the AV.

Next, inspired by the work in [40], we give a heuristic definition of the penalty vector  $\mathbf{h}$ :

*Definition 2:* The penalties for different distraction behaviors can be calculated in a probability perspective by:

$$\mathbf{h} := P(\text{damage}|\hat{\mathbf{c}}) \cdot \text{damage} \quad (6)$$

where  $\text{damage} \in \mathbb{R}^{N \times 1}$  denotes the normalized  $N$ -dimensional vector describing the  $N$  types of damage on personal safety, vehicles, mental-health and other aspects, and  $P(\text{damage}|\hat{\mathbf{c}}) \in \mathbb{R}^{K \times N}$  is the transition probability matrix with the item  $P(\text{damage}_i|\hat{c}_k)$  representing the probability of the  $i$ -th type of damage caused under the  $k$ -th distraction behavior.

Hence, the risk  $r_t$  can be computed by:

$$\begin{aligned} r_t &= r_{\text{norm}} \hat{\mathbf{c}}_t^T \cdot P(\text{damage}|\hat{\mathbf{c}}) \cdot \text{damage} \\ &= r_{\text{norm}} \sum_{k=1}^K \sum_{i=1}^N \hat{c}_{tk} \cdot P(\text{damage}_i|\hat{c}_{tk}) \cdot \text{damage}_i \end{aligned} \quad (7)$$

where  $P(\text{damage}_i|\hat{c}_{tk})$  can be calculated based on the statistics on the transition probabilities among the  $k$ -th distraction behavior, accident and the  $i$ -th type of damage as follows:

$$\begin{aligned} P(\text{damage}_i|\hat{c}_{tk}) &= P(\text{damage}_i|\text{distraction\_behaviour} = k, \text{accident} = \text{true}) \\ &\times P(\text{accident} = \text{true}|\text{distraction\_behaviour} = k) \end{aligned} \quad (8)$$

where  $\text{distraction\_behaviour} = k$  represents the driver stays in the  $k$ -th distraction behavior, and  $\text{accident} = \text{true}$  indicates that an accident exactly happens.

Note that the penalty vector  $\mathbf{h}$  can be computed and stored beforehand to support the calculation of the real-time risk caused by distraction behaviors. In fact,  $\mathbf{h}$  should also depend on factors such as speed and relative distance, since the risk caused by driver distraction behaviors differs a lot in different scenarios. For example, a small degree of distraction on high-speed expressways may lead to devastating damages compared to low-speed urban roads. Also, a small relative distance will increase the accident rate like rear-end collisions as well. Nevertheless, the more meticulous design of  $\mathbf{h}$  is beyond the scope of our paper, hence we make it constant for demonstration here.

Based on the above definitions and analysis, we can constrain the value range of  $r_t$  in the following corollary:

*Corollary 1:* The value of  $r_t$  can be constrained to  $[0,1]$  by setting  $r_{\text{norm}} = 1/\sqrt{K}$ , under the assumption that  $\hat{\mathbf{c}}_t^T \cdot \mathbf{1}_K = 1$ .

*Proof:* Please refer to Appendix VI.

### C. CONFIDENCE EVALUATION

In this subsection, we evaluate the confidence of the monitoring result based on the received sequences, to modify the influence of distraction behaviors along with the above-defined risk.

The reason to consider the confidence of the monitoring result is based on the fact that the behaviors of a driver are continuous and highly related in relatively small intervals on

the time horizon; however, the received results may suffer large fluctuations due to the noises at the part of V2V communications or even steep drops resulted from the temporal loss of the communication link. What's more, the misrecognition of the driver distraction would inevitably exist, and its effect should be weakened by the evaluated confidence. Hence, the introduction of confidence is much necessary which can improve the robustness of the influence evaluation of distraction behaviors.

The confidence evaluation is aimed to depict the generally negative correlation between the confidence and the difference between two adjacent monitoring results. Moreover, it should pay more attention to sharp fluctuations and be normalized. A simple example of the confidence  $\theta_t$  of the results  $\{\hat{\mathbf{c}}_t\}_{t \in \mathcal{T}}$  at time  $t \in \mathcal{T}$  could be set as  $\theta_t = \log(2 - \|\hat{\mathbf{c}}_t - \hat{\mathbf{c}}_{t-1}\|_2 / \sqrt{2}) / \log(2)$ . For demonstration, if we let  $\|\hat{\mathbf{c}}_t - \hat{\mathbf{c}}_{t-1}\|_2 = x$  and treat  $\theta_t$  as a function of  $x$ , namely we have  $\theta_t(x) = \log(2 - x/\sqrt{2}) / \log(2)$ , then we can demonstrate that for  $x \in [0, \sqrt{2}]$ : (1)  $\theta'_t(x) < 0$ ; (2)  $\theta''_t(x) < 0$  and (3)  $\theta_t(x) \in [0, 1]$ , which fits the design criterion well. Note that the difference will fall into the considered value range most of the time due to the intrinsic probability distribution property of  $\{\hat{\mathbf{c}}_t\}_{t \in \mathcal{T}}$ .

### D. INTEGRATING RISK AND CONFIDENCE INTO VELOCITY CONTROL

In this subsection, we integrate the risk and the corresponding confidence, which characterize the influence of the distraction behaviors of the human drivers, into the cost function of the temporal velocity control of the AV.

The cost function item at time  $t \in \mathcal{T}$  can be defined :

$$R_t = \theta_t \left( a_t - \left( r_t \left( -\frac{1}{\rho} \left( \frac{d_{\text{safe}}}{d_t^p - d_t} \right)^Q + \frac{1}{\rho} + 1 \right) + \rho \right) a_{\text{min}} \right)^2, \quad (9)$$

where  $a_{\text{min}}$  is the minimum acceleration of the AV, and  $d_{\text{safe}}$  is the minimum safe following distance, and  $Q > 0$  is used to modify the influence of relative distance on the risk, and  $\rho < 0$  standing for a stimulating parameter for acceleration when the preceding human drives safely. We could choose  $-\rho$  roughly equaling to the risk at the safe driving scenario, thus it could be regarded safe when the risk is lower than  $-\rho$ . It is noteworthy to point out that the term  $-\rho^{-1}(d_{\text{safe}}/(d_t^p - d_t))^Q + \rho^{-1} + 1$  could not only enlarge the risk when the relative distance drops below  $d_{\text{safe}}$  but also relieve potential conservative driving in the normal and low-risk driving conditions.

The design of  $R_t$  in (9) is mainly inspired by that an experienced driver will commonly make a strong brake when monitoring sudden emergency, hence we assume that the AV makes stronger brakes to deal with higher risk scenarios. What's more, the square constraint on  $a_t$  is adopted to make the subsequent optimization easily solvable and efficient.

Moreover, the influence of the risk is modified by the corresponding confidence  $\theta_t$ .

### E. SAFETY CONSTRAINTS

We analyze the safety constraints for the velocity control of the AV in this subsection.

Firstly, the control input of acceleration is bounded by the physical limitations on the actuators as:

$$a_{k|t} \in \mathcal{A} := \{x : a_{\min} \leq x \leq a_{\max}\}, \quad (10)$$

where  $a_{\min}$  and  $a_{\max}$  are the minimum and the maximum accelerations of the AV, respectively.

Then the speed limit of the AV leads to

$$v_{k|t} \leq v_{\max}. \quad (11)$$

More importantly, safe following distance should satisfy

$$d_{k|t}^p - d_{k|t} \geq d_{\text{safe}}(v_{k|t}), \quad \forall d_{k-1|t}^p \in \mathcal{A}^p, \quad (12)$$

where  $d_{\text{safe}}(v_{k|t})$  is the minimum safe following distance, being a function of the longitudinal velocity.

Nevertheless, it's extremely tough to deal with the above safe following constraint due to the uncertainty of the future acceleration of the human-driven vehicle  $d_{k|t}^p$  at time  $t$ . For robustness and simplicity, it's common to assume the worst case, namely the disturbance  $d_{k|t}^p$  takes on its lower bound  $d_{\min}^p$  at every time step in the prediction horizon  $[t, t + N_c - 1]$ . It's trivial that the constraint could be satisfied when the human-driven vehicle accelerates at a value greater than  $d_{\min}^p$ .

The predicted worst-case states of the human-driven vehicle, denoted by  $\bar{\xi}_{k|t}^p = [\bar{d}_{k|t}^p, \bar{v}_{k|t}^p]$ , are evolved as

$$\bar{\xi}_{k+1|t}^p = C\bar{\xi}_{k|t}^p + Da_{\min}^p. \quad (13)$$

Hence, the safety distance constraint can be turned to

$$\bar{d}_{k|t}^p - d_{k|t} \geq d_{\text{safe}}(v_{k|t}). \quad (14)$$

What's more, the satisfaction of (14) can ensure that of (12) since the adoption of the lower bound can lead to

$$\bar{d}_{k|t}^p \leq d_{k|t}^p, \quad \forall d_{k-1|t}^p \in \mathcal{A}^p. \quad (15)$$

The constraints (11) and (14) can be compactly expressed as:

$$g^\xi(\xi_{k|t}, \bar{\xi}_{k|t}^p) \leq 0. \quad (16)$$

By the same way, the constraint (10) can be expressed as:

$$g^a(a_{k|t}) \leq 0. \quad (17)$$

Moreover, from the safety aspect of the control system, the risk  $r_t$  and confidence  $\theta_t$  should both fall into reasonable ranges as well, leading to  $r_{k|t} \in \mathcal{R}$  and  $\theta_{k|t} \in \Theta$ . Here  $\mathcal{R}$  and  $\Theta$  are the value ranges of  $r_t$  and  $\theta_t$ , respectively.

By the same token, the constraints on  $r_{k|t}$  and  $\theta_{k|t}$  can be expressed as:

$$g^r(r_{k|t}) \leq 0 \quad (18)$$

and

$$g^\theta(\theta_{k|t}) \leq 0. \quad (19)$$

### F. PERSISTENT FEASIBILITY

In this subsection, we analyze the persistent feasibility of the safety constraints, which is of paramount importance to the practical AV control. It is easy to see that no guarantee exists to ensure the safety constraints (16)-(19) be satisfied in closed-loop. In general, to solve this, a suitably chosen target set (also often called terminal constraint set) is introduced to constrain the system state at the end of the horizon [30], [41]. Note that (18) and (19) can be guaranteed in closed-loop by the following evolutionary strategy of  $r_{k|t}$  and  $\theta_{k|t}$ .

*Remark 1:* To cater for the feedback mechanism of MPC, we assume that the distraction status of the human driver keeps same in the predicted time horizon, i.e.,  $r_{k+1|t} = r_{k|t}$  and  $\theta_{k+1|t} = \theta_{k|t}$  hold for  $k = 0, 1, \dots, N_c - 1$ .

Next, we adopt the popular method of invariant sets to compute the target set for the safety constraints (16) and (17) with persistent feasibility analysis. We first compute the maximal robust control invariant (RCI) set under the assumption that the preceding driver makes a strong brake in the predicted horizon. Then we use a recursive strategy to compute the polyhedral target set for the safety constraints at the end of the horizon.

Before proceeding to the computation of maximal RCI set, we introduce the definition of RCI set and maximal RCI set as below, respectively:

*Lemma 1:* Consider the system  $x_{t+1} = f(x_t, u_t, w_t)$ , where the state  $x_t \in \mathcal{X}$ , the input  $u_t \in \mathcal{U}(x)$  and the disturbance  $w_t \in \mathcal{W}(x, u)$ . A set  $X_f \subseteq \mathcal{X}$  is said to be an RCI set for the system if

$$\begin{aligned} x_t \in X_f \\ \implies \exists u_t \in \mathcal{U}(x) \text{ s.t. } f(x_t, u_t, w_t) \in X_f \quad \forall w_t \in \mathcal{W}(x, u). \end{aligned} \quad (20)$$

*Lemma 2:* The RCI set which contains all other RCI sets is called the maximal RCI set.

From Lemma.1, in our case, we can get the state  $x_t = [\xi_t, \xi_t^p, r_t, \theta_t]$ , the input  $u_t = a_t$  and the disturbance  $w_t = d_t^p$  for the AV. Note that the evaluated risk  $r_t$  and confidence  $\theta_t$  are also included in the state of the system.

To compute the maximal RCI set, we assume that the preceding human driver makes the maximum brake since time  $t$  with system state  $\xi_t^p = [d_t^p, v_t^p]$ . It will be demonstrated that this is sufficient to compute the required RCI set. It is then assumed that after  $t_s$  time interval, the preceding vehicle stops. Hence, we can have  $\bar{v}_{k|t}^p = 0$  for  $k \geq t_s$ . And the maximal RCI set  $X_S$  for the predicted AV state at time  $(t + t_s)$  can be computed as follows:

$$\begin{aligned} X_S = \{ & [\xi_{t_s|t}, \bar{\xi}_{t_s|t}^p, r_{t_s|t}, \theta_{t_s|t}] \exists a_{t_s|t} \\ \text{s.t. } & [\xi_{t_s+1|t}, \bar{\xi}_{t_s+1|t}^p, r_{t_s+1|t}, \theta_{t_s+1|t}] \in X_S, \\ & \xi_{t_s+1|t} = C\xi_{t_s|t} + Da_{t_s|t}, \bar{\xi}_{t_s+1|t}^p = \bar{\xi}_{t_s|t}^p, \\ & g^r(r_{t_s|t}) \leq 0, g^\theta(\theta_{t_s|t}) \leq 0, \\ & g^a(a_{t_s|t}) \leq 0, g^\xi(\xi_{t_s|t}, \bar{\xi}_{t_s|t}^p) \leq 0\}. \end{aligned} \quad (21)$$

To compute  $X_s$ , we could adopt the Multi-Parametric Toolbox (MPT) in MATLAB.

Next, we utilize the recursive strategy to compute the target set  $X_f$  at the end of the predicted horizon time  $t + N_c$ . Central to the computation is the commonly used predecessor set (or one-step backward reachable set) of a given set as follows [41]:

*Lemma 3:* Given a set  $\Omega \subseteq \mathcal{X}$ , the predecessor set  $\text{Pre}(\Omega)$  is the set of states for which there exists an admissible input such that, for all allowable disturbances, the successor state is in  $\Omega$ , i.e.,

$$\text{Pre}(\Omega) := \{x_t | \exists u_t \in \mathcal{U}(x) \\ \text{s.t. } f(x_t, u_t, w_t) \in \Omega, \forall w_t \in \mathcal{W}(x, u)\}. \quad (22)$$

To compute the target set  $X_f$  at time  $t + N_c$  based on the set  $X_s$  at time  $t + t_s$ , a recursive strategy can be utilized for the  $(t_s - N_c)$ -step backward reachable set. Note that here we only consider the case that  $t_s > N_c$ , since if  $t_s \leq N_c$ , that  $X_f = X_s$  is sufficient to guarantee the persistent feasibility of the MPC problem.

In our case, the predecessor set takes the following form:

$$\text{Pre}(\Omega) = \{[\bar{\xi}_{k|t}, \bar{\xi}_{k|t}^p, r_{k|t}, \theta_{k|t}] | \exists a_{k|t} \\ \text{s.t. } [\bar{\xi}_{k+1|t}, \bar{\xi}_{k+1|t}^p, r_{k+1|t}, \theta_{k+1|t}] \in \Omega, \\ \bar{\xi}_{k+1|t} = C\bar{\xi}_{k|t} + Da_{k|t}, \\ \bar{\xi}_{k+1|t}^p = C\bar{\xi}_{k|t}^p + Da_{k|t}^p, \\ g^r(r_{k|t}) \leq 0, g^\theta(\theta_{k|t}) \leq 0, \\ g^a(a_{k|t}) \leq 0, g^\xi(\bar{\xi}_{k|t}, \bar{\xi}_{k|t}^p) \leq 0\}. \quad (23)$$

*Remark 2:* The  $(t_s - N_c)$ -step backward reachable set of  $X_s$ ,  $X_{t_s - N_c}$ , can be computed recursively :

$$X_{j+1} = \text{Pre}(X_j), \quad j = 0, 1, \dots, t_s - N_c - 1, X_0 = X_s. \quad (24)$$

Finally, we can get the following theorem of the target set  $X_f$  for the MPC problem.

*Theorem 1:* Let  $X_f$  be the  $(t_s - N_c)$ -step backward reachable set to  $X_s$ , namely  $X_f = X_{t_s - N_c}$ , and the MPC problem can be persistently feasible with respect to the safety constraints (16)-(19) if it is satisfied that  $[\bar{\xi}_{N_c|t}, \bar{\xi}_{N_c|t}^p, r_{N_c|t}, \theta_{N_c|t}] \in X_f$ .

*Proof:* On the one hand, it is trivial to prove that the safety constraints (18) and (19) can be guaranteed in closed-loop based on the evolutionary strategy shown in Remark 1.

On the other hand, the proof for (16) and (17) can be completed from three value ranges of  $k$ . Firstly, (16) and (17) can be trivially proved to hold for  $k \in [0, N_c - 1]$  based on  $[\bar{\xi}_{N_c|t}, \bar{\xi}_{N_c|t}^p, r_{N_c|t}, \theta_{N_c|t}] \in X_f$  and the recursive strategy. Then, for  $k \in [N_c, t_s - 1]$ , since  $X_f = X_{t_s - N_c}$ , there exists a feasible sequence of control inputs  $\{a_{k|t}\}_{k=N_c}^{t_s-1}$  such that  $\{[\bar{\xi}_{k|t}, \bar{\xi}_{k|t}^p, r_{k|t}, \theta_{k|t}]\}_{k=N_c}^{t_s-1}$  satisfy (16) and (17) and  $[\bar{\xi}_{t_s|t}, \bar{\xi}_{t_s|t}^p, r_{t_s|t}, \theta_{t_s|t}] \in X_s$  for  $d_{k|t}^p = d_{\min}^p$ . Finally, for  $k \geq t_s$ , (16) and (17) can be guaranteed resulting from the definition of  $X_s$ . Considering here we adopt the  $d_{\min}^p$  to get the

worst-case for the preceding vehicle, the safety constraints can be naturally held for all possible  $d_{k|t}^p \in \mathcal{A}^p$  for  $k \in \mathbb{N}_+$ .

In summary, the safety constraints (16)-(19) can be guaranteed in closed-loop for all possible  $d_{k|t}^p \in \mathcal{A}^p$  for  $k \geq 0$ , and the proof is completed.

### G. MPC FORMULATION

In this subsection, we formulate the optimization problem based on MPC strategies as well as the aforementioned constraints.

First of all, in practice, the safety distance constraint (14) is usually imposed as a soft constraint with a high penalty  $P$  on the constraint violation  $\epsilon$  in the following equation, which aims to guarantee the AV never collide with the preceding vehicle:

$$\bar{d}_{k|t}^p - d_{k|t} \geq d_{\text{safe}}(v_{k|t}) - \epsilon, \quad \epsilon \geq 0. \quad (25)$$

Also, the initial conditions for the state and the input are :

$$\bar{\xi}_{0|t} = \xi_t, \quad \bar{\xi}_{0|t}^p = \xi_t^p, \quad r_{0|t} = r_t, \quad \theta_{0|t} = \theta_t \quad (26)$$

and

$$a_{-1|t} = a_{t-1}. \quad (27)$$

Then we define the cost function by introducing a control horizon  $N_c$  into the online optimization :

$$G = \sum_{k=t}^{t+N_c-1} [R_k + \alpha(a_k - a_{k-1})^2 + \beta(v_{\max} - v_k)], \quad (28)$$

where  $\alpha$  and  $\beta$  are parameters penalizing the jerk and the deviation from the speed limit, respectively.

Finally, the sequence of control input  $\mathbf{a}_t = [a_{0|t}, \dots, a_{N_c-1|t}]$  is computed as the solution of the following constrained finite-time optimal control problem:

$$\min_{\mathbf{a}_t} G + P\epsilon \quad (29a)$$

$$\text{s.t. } \bar{\xi}_{k+1|t} = C\bar{\xi}_{k|t} + Da_{k|t} \quad (29b)$$

$$\bar{\xi}_{k+1|t}^p = C\bar{\xi}_{k|t}^p + Da_{k|t}^p \quad (29c)$$

$$r_{k+1|t} = r_{k|t}, \quad \theta_{k+1|t} = \theta_{k|t} \quad (29d)$$

$$g^\xi(\bar{\xi}_{k|t}, \bar{\xi}_{k|t}^p) \leq \epsilon \quad (29e)$$

$$g^a(a_{k|t}) \leq 0 \quad (29f)$$

$$g^r(r_{k|t}) \leq 0 \quad (29g)$$

$$g^\theta(\theta_{k|t}) \leq 0 \quad (29h)$$

$$[\bar{\xi}_{N_c|t}, \bar{\xi}_{N_c|t}^p, r_{N_c|t}, \theta_{N_c|t}] \in X_f \quad (29i)$$

$$\bar{\xi}_{0|t} = \xi_t, \quad \bar{\xi}_{0|t}^p = \xi_t^p \quad (29j)$$

$$r_{0|t} = r_t, \quad \theta_{0|t} = \theta_t \quad (29k)$$

$$a_{-1|t} = a_{t-1}. \quad (29l)$$

Importantly, the above optimization problem (29) is a quadratic program that can be solved efficiently in real time, which can make the formulation much practical. What's more, the intrinsic feature of MPC which only adopts the current computed acceleration  $a_{0|t}$  but based on the prediction over the time horizon  $N_c$  could provide more robustness to the control system [42], [43].

#### IV. BENEFIT ANALYSIS OF COLLABORATIVE FRAMEWORK

In this section, we analyze and visualize the safety benefits our collaborative framework could help improve, where the AV takes into consideration distraction behaviors of the preceding human driver, by comparing the increase of safety regions with and without our collaborative framework on the condition of preserving the traffic performance.

As demonstrated by numerous accidents, distraction will definitely lead to a decrease of the driving ability of drivers. As a result, it is not uncommon that the driver makes a strong brake to deal with the sudden emergency when turning back from distraction, which will largely increase the probability of rear-end collisions for the following vehicles. On the other hand, with the help of our collaborative framework, the AV can predict the potential risks over the predicted time horizon based on the real-time driver distraction monitoring and spare more space to avoid rear-end collisions. What's more, instead of too cautiously making strong brakes to avoid distracted drivers, our framework can preserve the traffic performance by adaptive velocity control based on real-time monitored results. Next, we make safety analysis to indicate the benefits of our collaborative framework.

For demonstration, we consider the car-following scenario and compare the final relative distances resulted from two schemes: one without our framework that the AV brakes after receiving the brake signal from the preceding vehicle, and the other which allows the AV to predict the potential risks based on distraction monitoring and V2V communications and decelerate in advance. For brevity, we assume that the driver falls into distraction during time  $i$  to time  $j$  ( $i < j$ ) with unit time interval we concerned and makes a strong brake with  $a_{\min}$  to deal with the sudden emergency at time  $j$ , where  $a_{\min}$  is the minimum acceleration for both the human-driven vehicle and the AV. Moreover, as we know, both the V2V communication latency and the delay caused by driver distraction detection will postpone the following AV's actions. Hence, we assume the V2V communication delay is  $\tau$  for both transmission of distraction information and spreading of braking information, and the delay caused by online distraction detection is  $\mu$ . In addition, no matter whether the collaborative framework is utilized, the AV needs an operation time  $\eta$  to take control actions once receiving signals. When the AV detects the distraction of the driver, it brakes with  $\{a_t\}_{t=i+\mu+\tau+\eta}^{j+\tau+\eta-1}$  where  $a_t < 0$  to spare more space for safety from time  $i + \mu + \tau + \eta$  to time  $j + \tau + \eta - 1$ , and then brakes with  $a_{\min}$  at time  $j + \tau + \eta$  when detecting the sudden strong brake of the driver.

For initial conditions and constraints, we assume  $v_i = v_i^p = v_0$  and  $d_i^p - d_i = \delta_0$ , and suppose that  $j > i + \mu$  and  $v_0 > \sum_{t=i+\mu+\tau+\eta}^{j+\tau+\eta-1} |a_t|$  to ensure that the AV is not too conservative to stop before the driver's vehicle stops. Based on the analysis, we arrive at the following theorem on final relative distance:

*Theorem 2:* Considering the car-following scenario as shown in Fig. 1, with the assistance provided by the collaborative framework, the following AV can predict the risks based on the real-time distraction monitoring of human driver and decelerate in advance, thus the final relative distance can be increased from  $\delta_0 - v_0\tau - v_0\eta$  to at least following  $\underline{\delta}_{\text{stop}}$ :

$$\underline{\delta}_{\text{stop}} = \delta_0 - v_0\tau - v_0\eta + \frac{|a_{\text{ave}}|}{|a_{\min}|}v_0(j - i - \mu) + \frac{1}{2}|a_{\text{ave}}|\left[1 - \frac{|a_{\text{ave}}|}{|a_{\min}|}\right](j - i - \mu)^2, \quad (30)$$

where  $a_{\text{ave}}$  is the average acceleration of  $\sum_{t=i+\mu+\tau+\eta}^{j+\tau+\eta-1} |a_t|$ , namely  $a_{\text{ave}} = \sum_{t=i+\mu+\tau+\eta}^{j+\tau+\eta-1} |a_t| / (j - i - \mu)$ .

*Proof:* Please refer to Appendix VI.

*Remark 3:* From the above theorem, we can conclude that without our collaborative framework, it may cause rear-end collision if  $\delta_0 < v_0(\tau + \eta)$ , for example in the cases of high speeds or small relative distances. Nevertheless, our framework can increase the relative distance by  $|a_{\text{ave}}|/|a_{\min}|v_0(j - i - \mu) + 1/2|a_{\text{ave}}|[1 - |a_{\text{ave}}|/|a_{\min}|](j - i - \mu)^2$  through predicting the potential risks and decelerating in advance, which can definitely spare more space to reduce the probability of rear-end collisions.

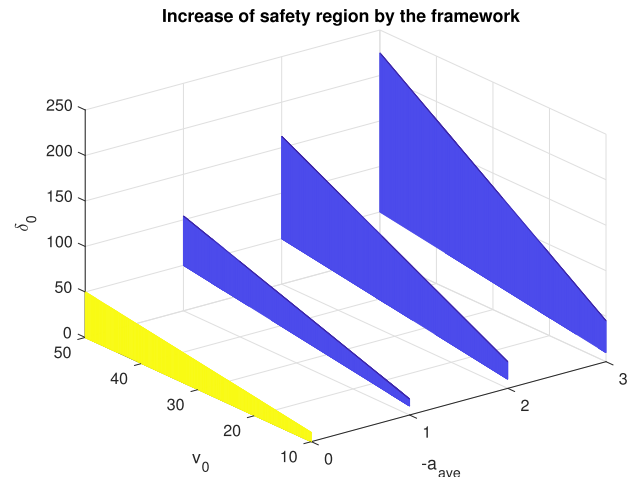


**FIGURE 2.** Demonstration of the increase of safety region resulted from the framework for  $a_{\text{ave}} = 0, 1, 2, 3 \text{ m}^2/\text{s}$  with  $\tau = \mu = \eta = 0.5 \text{ s}$ .

To demonstrate the safety region explicitly, we assume the final relative distance  $\delta_{\text{stop}} = 0$ , and come to the safety regions for the initial speed  $v_0$  and initial relative distance  $\delta_0$  which can avoid the rear-end collision in Fig. 2. From Fig. 2, we can see that the initial safety region in yellow is very restricted, while our framework can increase it by blue regions to provide safer situations.

#### V. SIMULATIONS

In this section, we have implemented two simulations to illustrate the feasibility of our collaborative framework and its

efficacy at increasing the safety of transportation networks: the contrast tests of real-time evaluation of driver distraction monitoring and the longitudinal velocity control strategy of AV, both on a server with two 2.10 GHz Intel(R) Xeon(R) E5-2620 CPUs (each contains six cores) and 64 GB RAM.

**A. REAL-TIME EVALUATION OF DISTRACTION MONITORING**

In this subsection, we provide a real-time driver distraction monitoring implementation based on convolutional neural networks (CNNs), which have been validated as one type of neural networks powerful in detection and recognition of objects and regions in images. First, we introduce the data which is originated from reality, followed by several pre-processing steps. Then we explain our CNN model. Finally, we evaluate the online processing of our model and analyze the tradeoff between the time cost and the performance under different configuration conditions.

**1) DATA AND PREPROCESSING**

To be convinced, we adopted the real-world data from a public competition of State Farm [44], which aims to improve alarming statistics and better ensure the customers, by testing whether dashboard cameras can automatically detect drivers engaging in distracted behaviors. The task is to classify each driver’s behaviors such as whether they are driving attentively, wearing their seatbelt, or taking a selfie with their friends in the backseat.

We used about 4000 labeled images in the data for training, and 2000 labeled images for testing with the size of each image being  $640 \times 480$  pixels. Labeled images were divided into 10 classes from c0 to c9 as explained in Table 1, where only c0 denotes safe driving state, while others referring to various distraction behaviors.

**TABLE 1. Classification of human driver’s distraction behaviors.**

Class	Content	Class	Content
c0	safe driving	c5	operating the radio
c1	texting-right	c6	drinking
c2	talking on the phone-right	c7	reaching behind
c3	texting-left	c8	hair and makeup
c4	talking on the phone-left	c9	talking to passenger

Before moving on to the CNN model, several preprocessing steps were in order. To accelerate the processing and cater for the  $8 \times 8$ -dimension convolutional filters used in the sequel, we resized the images from  $640 \times 480$  to common  $64 \times 64$ . What’s more, note that the raw input is redundant since adjacent pixel values are highly correlated [45]. Therefore, we used ZCA whitening to make the input less redundant, before which local mean subtraction was adopted as well.

**2) CNN MODEL FOR DISTRACTION MONITORING**

The visualized CNN model for distraction monitoring is shown in Fig. 3. It includes one linear decoder and one CNN

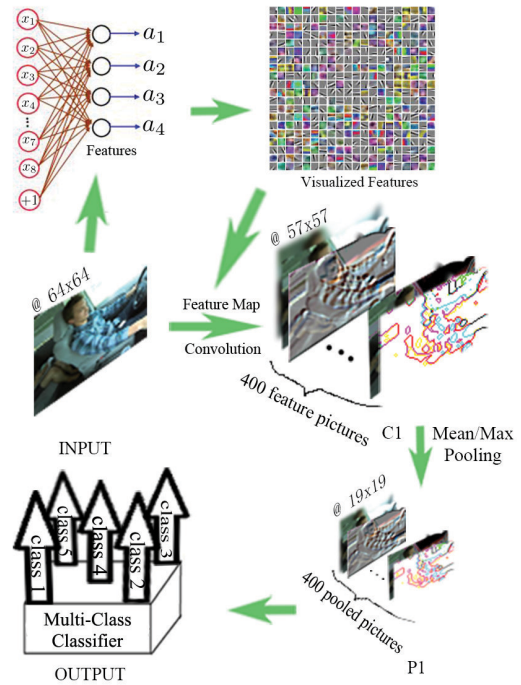


**FIGURE 3. CNN model for distraction monitoring.**

of three layers (the first INPUT layer excepted): one convolutional layer marked as C1, one pooling layer marked as P1, and one OUTPUT layer. Notice that other than training the CNN based on the raw input directly, here we introduced the unsupervised learning to improve the efficiency of learning higher-level features based on the lower-level features learned in advance. We implement the CNN model in MATLAB, mainly based on the CNN module of “UFLDL tutorial” [45].

First of all, the  $8 \times 8$ -dimensional color features were learned as the convolutional filters used in the sequel. Here we utilized 400 hidden units in the linear decoder to learn the 400 filters, which lead to 400 feature maps (namely the map from the input layer to the hidden layer) at the C1 layer. In more detail, for the linear decoder part, we assumed a more general scenario where unlabeled data set do not have the same distribution with the training data set, such that self-taught learning was used to finish the learning of color features. We used 100,000 small  $8 \times 8$ -dimensional patches sampled from the public STL-10 dataset [46], which contains 10 classes of colorful images including airplanes, birds and cars and so on, to learn 400 color features. Hence, the linear decoder had 400 hidden units. It was trained for 400 iterations and the learned color features were shown in Fig. 3. It’s noteworthy that if the unlabeled data has the same distribution with the training data set, the semi-supervised learning may result in color features more suitable for the specific task in practical applications. For the supervised learning part, we adopted a scaled sigmoid activation function for the C1 layer and a linear activation function for the P1 layer, and a softmax activation function for the OUTPUT layer. The training of the parameters utilized online gradient descent

with a learning rate. During the training, images were continually translated, scaled and rotated, whereas only the original images were used for validation. The training phase ended once the validation error was small enough (for example below 0.001) or when the learning rate reached its pre-determined minimum or the number of iterations reached its maximum. The initial weights were drawn from a uniformly random distribution in the range  $[-0.05, 0.05]$ .

Then, at the C1 layer, every  $64 \times 64$ -dimensional image passed through  $400 \ 8 \times 8$ -dimensional filters and generated  $400 \ 57 \times 57$ -dimensional feature pictures (57 resulted from the convolution operation). At the subsequent P1 layer,  $3 \times 3$ -dimensional mean pooling method was adopted to generate  $400 \ 19 \times 19$ -dimensional pooled pictures.

Finally, at the OUTPUT layer, the softmax classifier was employed as the multi-class classifier. It generated a 10-dimensional vector to present the probability predicted for each class, which corresponds to the 10 classes of distraction behaviors of drivers.

After the training of the CNN model, all the parameters including weights and biases will be stored offline. As for the real-time monitoring, the pictures of the drivers will be captured online with a predefined time interval and be input into the trained CNN model one by one, and then the processor returns the classification results after acceptable delays.

### 3) CONTRAST TESTS UNDER DIFFERENT CONDITIONS

After the CNN model being trained, we stored all the parameters offline and sent the images from the test data set one by one to the trained CNN model (with trained convolutional filters), then we calculated the time cost of the processing. Afterward, we analyzed the time cost and performance under different conditions. We also used “parfor-loop” instead of “for-loop” on the MATLAB platform to parallelize the procedure of pooling and convolution.

**TABLE 2. Accuracy and time when varying the number of layers.**

Pooling size	Number of Layers	Accuracy	Time
$3 \times 3$	7	96.48%	3.58 s
$3 \times 3$	5	95.23%	1.23 s
$3 \times 3$	3	92.45%	0.27 s
$3 \times 3$	1	82.26%	0.16 s

**TABLE 3. Accuracy and time when varying pooling size.**

Pooling size	Number of Layers	Accuracy	Time
$1 \times 1$	3	94.36%	1.03 s
$3 \times 3$	3	92.45%	0.27 s
$8 \times 8$	3	72.38%	0.14 s

As shown in Table 2, more layers lead to higher accuracy without overfitting at the cost of more time, which fits the intuition well. Though not revealed in the table, overfitting still appeared when we increased the iterations or reduced the error rate during the training. The impact of pooling size is shown in Table 3. We can see that larger pooling sizes lead to

**TABLE 4. Accuracy and time when disabling the parallelization.**

Number of Layers	Parallelized	Accuracy	Time
3	yes	92.45%	0.27 s
3	no	91.98%	1.03 s

faster processing but lower accuracy, which is resulted from the coarser characterization of the convolutional pictures. Table 4 reveals a distinct improvement of the adoption of the parallelization of convolution and pooling under the same  $3 \times 3$  pooling size. Note that the classification accuracy would affect the AV control performance. For instance, misrecognizing distraction as safe driving, namely the true negative cases, would lead to aggressive driving of the AV. Inversely, regarding safe driving as distraction would induce cautious driving. Moreover, in the case of misrecognizing one type of distraction as another type of distraction, the influence on the risk could be constrained which is only resulted from the different weights of the penalty vector  $h$ . Hence, besides the improvement of hardware resources and the algorithms at the distraction monitoring part, from the viewpoint of the whole control system, it is necessary to introduce the confidence evaluation on the classification results to improve the safety, as shown in Section III-C.

These contrast tests under different configuration conditions can give guidance to modify the CNN model according to the available hardware resources. For example, in our experiments, the case with three layers and pooling size of  $3 \times 3$  and parallelization being adopted is suitable since the classification accuracy can achieve 92.45% in less than 0.3 s.

### B. VELOCITY CONTROL OF AV

In this subsection, we simulated two common scenarios to show the advantages the collaborative framework can bring to the AV: avoiding the distracted driver and reducing rear-end collision, thus we can mark the two scenarios as cautious-avoidance scenario and collision-reduction scenario, respectively. Note that our collaborative framework can preserve the traffic performance as much as possible by adaptively anticipatory velocity control other than too cautiously strong brakes to avoid the potentially distracted drivers.

For demonstration, we took the following particular situation as an example of the cautious-avoidance scenario that the preceding driver fell into two types of distractions: talking on the phone at right (c2) then reaching behind (c7) with a constant speed, and as a result, the AV drove more cautiously to spare more relative distance to avoid the driver. The second scenario was that the driver made a strong brake to handle the sudden emergency when texting on the phone at left (c3), which might divert the driver’s attention severely from visual, cognitive and manual aspects. Moreover, here we made comparisons with the case without the collaborative framework on the assumption that the AV could make strong brakes with a delay when detecting the brake signal of the preceding vehicle.

TABLE 5. Control design parameters.

Parameter	Value	Parameter	Value
$\Delta t_c$	0.2 s	$T_c$	2.6 s
$\alpha$	4e-3	$T$	12 s
$\beta$	3e-1	$a_{min}$	-8 m/s <sup>2</sup>
$P$	5000	$a_{max}$	8 m/s <sup>2</sup>
$\rho$	-0.1	$v_{max}$	30 m/s
$r_{norm}$	7/√10	$Q$	0.1

In detail, we assumed that the initial relative distance between the AV and the human-driven vehicle was 17 m, and the minimum safe following distance  $d_{safe}(v) = 0.5v + 5$ . The initial speeds of both were 20 m/s, and the initial acceleration of the AV was 0 m/s<sup>2</sup>. What’s more, based on the statistical results on crash risk associated with driver distraction in [47] and [48] and how many of the three aspects (visual, cognitive and manual) [49] would be affected by the distraction behavior, we assumed a normalized penalty vector  $\mathbf{h} = [7.56e - 05, 0.60, 0.23, 0.60, 0.23, 0.076, 0.076, 0.38, 0.076, 0.076]^T$  for demonstration, which could be further modified based on more experimental data according to the probabilistic method mentioned in Part III-B. Other parameters used in the control design are listed in Table 5, where  $T$  stands for the whole control time and is aimed to offer a longer observation time for the AV’s adaptive control. It’s noteworthy that the collaborative framework could provide similar results with the parameters of other reasonable values.

In the cautious-avoidance scenario, to simulate the preceding driver falling into the states, talking on the phone at the right side (c2) then reaching behind (c7), we generated the received monitoring results  $\{\hat{c}_i\}_{i=1}^{t=40}$  with safe driving (c0) in the majority while talking on the phone at the right side from 0.8 s to 2 s and reaching behind from 4 s to 5.6 s, where the process was simulated by a predetermined quadratic concave function. Also, the monitoring result at each time was scaled to satisfy that the summation of all elements equaled to 1. Moreover, we assumed the driver drove at a constant speed without coming across emergencies. What’s more, to be practical, more operational details should be taken into consideration, like the time consumption for V2V communications, image processing, and vehicle’s mechanical operations. Therefore, we made assumptions that the V2V communication delays for both transmissions of distraction information and braking information, as well as the delay caused by online distraction detection and the AV’s mechanical operation time, were all 0.4 s, compared to which the time on the evaluations of the risk and the confidence at the AV side could be neglected. Thus, the received monitoring results, the risk evaluation, and the confidence evaluation all have a 0.8 s delay and the AV control has a 1.2 s delay. The simulated results can be visualized in Fig. 4 with c0, c2 and c7 in bold. Based on the received monitoring results, the sequences of risk and confidence can be evaluated by Equation (5) and the example function in Section III-C. As shown in Fig. 5, the risk caused by reaching behind is higher than talking

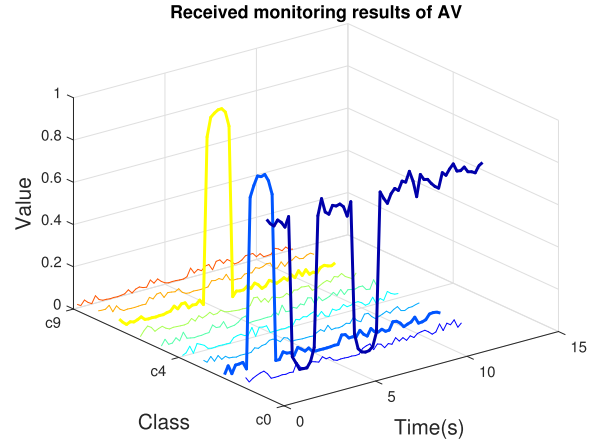


FIGURE 4. Visualization of the received monitoring results of AV in the cautious-avoidance scenario.

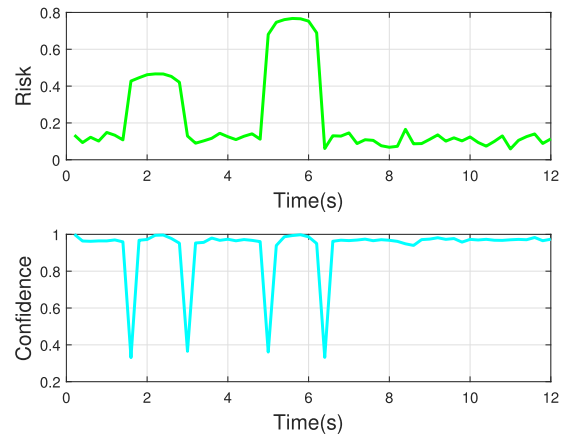


FIGURE 5. Risk and confidence evaluation in the cautious-avoidance scenario.

on the phone at the right side due to a bigger penalty value in  $\mathbf{h}$ , and the confidence stays stationary except distraction appearing or ending, which fits the intuition well.

To deal with the distracted preceding driver, the AV chose to drive more cautiously to avoid the driver. In detail, the AV could adaptively adjust its speed according to the real-time predicted risks and confidence as shown in Fig. 6. As a result, the AV can spare more relative distance in case that the preceding distracted driver makes suddenly strong brakes to handle emergencies. Note that the AV could also apply large accelerations and return to its available maximum speed gradually as long as the relative distance is safe.

In the collision-reduction scenario, the preceding driver was assumed texting on the phone at left (c3) since 0.8 s with a constant speed, then monitoring an emergency like that a pedestrian suddenly appeared, thus making a strong brake at 2.6 s. Here compared to the cautious-avoidance scenario, the driver no more drove at a constant speed while making brakes to handle emergencies. Considering the delays of V2V communications and online distraction detection and the AV’s mechanical operation time, the AV cautiously avoid

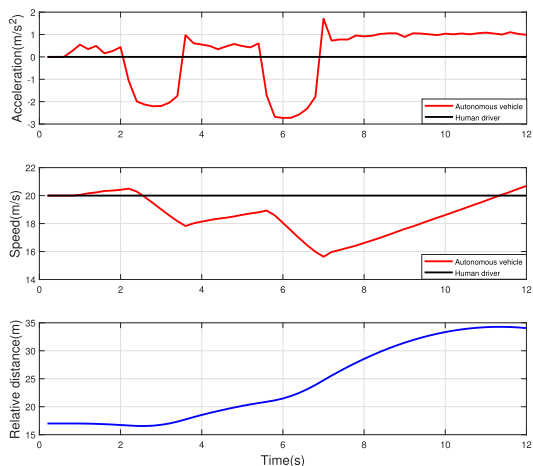


FIGURE 6. Velocity control of AV in the cautious-avoidance scenario.

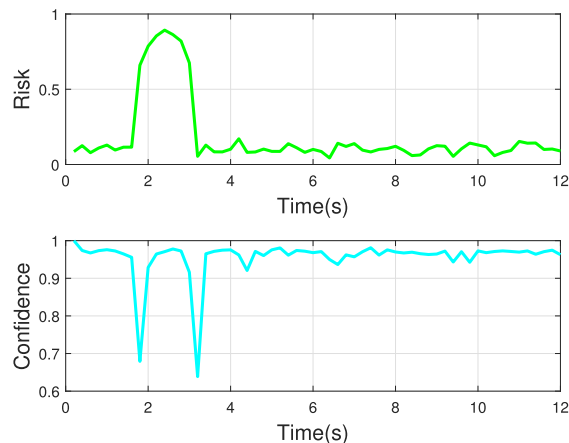


FIGURE 8. Risk and confidence evaluation in the collision-reduction scenario.

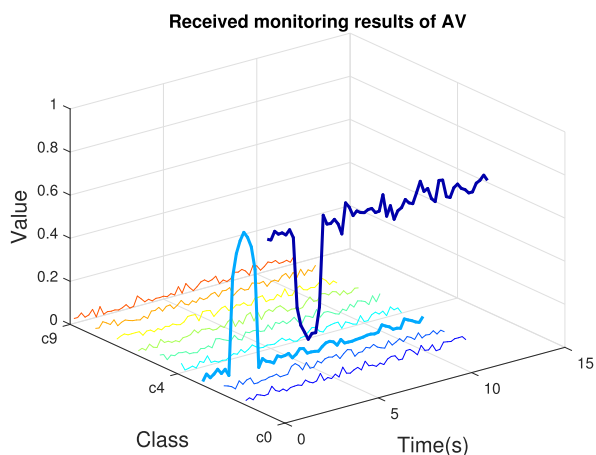


FIGURE 7. Visualization of the received monitoring results of AV in the collision-reduction scenario.

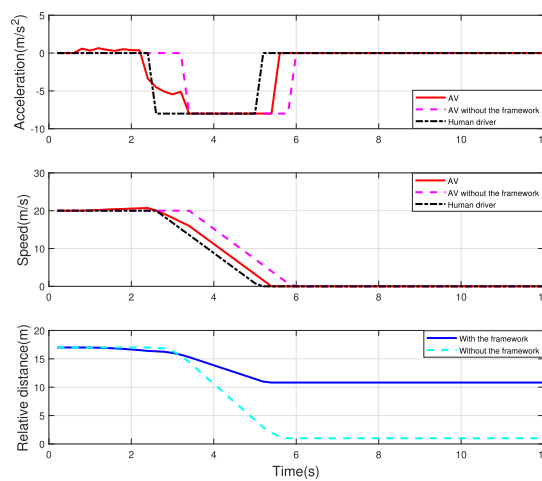


FIGURE 9. Velocity control of AV in the collision-reduction scenario.

the distracted driver since 2 (resulted from  $0.8 + 0.4 + 0.4 + 0.4$ ) s, and make strong brakes at 3.4 (resulted from  $2.6 + 0.4 + 0.4$ ) s once receiving the brake signals from the preceding human-driven vehicle, as same as the analysis in the above section. Note that we assume the AV control system could adopt the minimum value between the current computed acceleration of MPC and the received acceleration value from the preceding human-driven vehicle, which is practical to keep safe in case of emergency. And the monitoring system will be kept on until the AV totally stops, thus the AV could resume to the normal driving scenario when the risk goes away as long as it's not fully stopped. As a result, Fig. 7 shows the received monitoring results by the AV in the collision-reduction scenario. Subsequently, the risk and confidence are demonstrated in Fig. 8. For the velocity control of the AV, from Fig. 9, we can see that the AV can predict the potential risks and spare more relative distance with the driver falling in distractions. On the other hand, the AV's adaptively anticipatory velocity control can preserve the traffic performance as much as possible other than too cautiously making strong brakes once detecting distraction

behaviors. To further demonstrate the effectiveness of our framework, we also simulated the actions of the AV without our collaborative framework, namely making brakes at 3.4 s once received the brake signals from the preceding human-driven vehicle. From the simulation results, we can show that our collaborative framework can help the AV reduce the rear-end collision to some extent. To go a further step, considering the delays, the framework could take effect if the time interval exceeds 1.2 s between the start of distraction and the strong brake of the human driver.

In summary, we can conclude from the experiments that the AV equipped with our collaborative framework can drive more cautiously to avoid the distracted driver and reduce the collisions in the case of sudden brakes.

## VI. CONCLUSION

This paper focuses on how the AV could make smart longitudinal velocity control to deal with the vehicle driven by a distracted human driver. To achieve the goal, we put forward a practical collaborative framework to integrate data acquisition and processing, V2V communications, and the

AV control from both the human driver side and the AV side. Then, to utilize the driver's distraction information effectively, we propose a method of longitudinal velocity control for the AV based on MPC strategies, considering the risk and the confidence of driver distraction behaviors. Furthermore, we analyze and visualize the safety benefits the collaborative framework could help improve. The simulations show that the driver distraction monitoring implementation based on the CNN can be approximately real-time which can achieve 92.45% accuracy in less than 0.3 s; and our velocity control method is efficacy at guiding the AV to act smartly to predict the risks caused by the driver's distraction and improve its safety by cautiously avoiding distracted drivers and reducing rear-end collisions.

**APPENDIXES**

**APPENDIX A**

**PROOF OF COROLLARY 1**

Recall (7):

$$r_t = r_{\text{norm}} \hat{c}_t^T \cdot P(\text{damage}|\hat{c}) \cdot \text{damage}. \quad (31)$$

Thus, we have

$$\begin{aligned} |r_t| &= |r_{\text{norm}} \hat{c}_t^T \cdot P(\text{damage}|\hat{c}) \cdot \text{damage}| \\ &\leq |r_{\text{norm}}| \cdot \|\hat{c}_t^T\|_2 \cdot \|P(\text{damage}|\hat{c})\|_F \cdot \|\text{damage}\|_2 \end{aligned} \quad (32)$$

Next, we compute the value range of  $\|\hat{c}_t^T\|_2$ . Since  $\hat{c}^T \in \mathbb{R}_+^K$ , it is trivial to get

$$\cos(\text{angle}(\hat{c}^T, \mathbf{1})) \in [1/\sqrt{K}, 1] \quad (33)$$

Then based on  $\hat{c}^T \cdot \mathbf{1}_K = 1$ , we have

$$\|\hat{c}^T\|_2 \cdot \|\mathbf{1}\|_2 \cdot \cos(\text{angle}(\hat{c}^T, \mathbf{1})) = 1 \quad (34)$$

Hence, we can have  $\|\hat{c}_t^T\|_2 \in [1/\sqrt{K}, 1]$ .

Then we compute the value range of  $\|P(\text{damage}|\hat{c})\|_F$ .

First, we have

$$\begin{aligned} &\|P(\text{damage}|\hat{c})\|_F \\ &\stackrel{(a)}{=} \sqrt{\text{tr}(P(\text{damage}|\hat{c})P^T(\text{damage}|\hat{c}))} \\ &\stackrel{(b)}{=} \sqrt{\sum_{i=1}^N \sum_{k=1}^K P(\text{damage}_i|\hat{c}_k)^2} \\ &\stackrel{(c)}{=} \sqrt{\sum_{k=1}^K \|P(\text{damage}|\hat{c}_k)\|_2^2} \end{aligned} \quad (35)$$

where  $P(\text{damage}|\hat{c}_k)$  presents the  $k$ -th row of  $P(\text{damage}|\hat{c})$ , and the derivation (a), (b) and (c) result from the definition of Frobenius norm, matrix trace and 2-norm, respectively.

Moreover, due to the definition of  $P(\text{damage}_i|\hat{c}_k)$  in Definition. 2, we can have the following property of  $P(\text{damage}|\hat{c}_k)$ :

$$P(\text{damage}|\hat{c}_k) \cdot \mathbf{1}_N = 1 \quad (36)$$

and

$$P(\text{damage}|\hat{c}_k) \in \mathbb{R}_+^N. \quad (37)$$

By the same analysis of  $\hat{c}_t^T$ , we can have  $\|P(\text{damage}|\hat{c}_k)\|_2 \in [1/\sqrt{N}, 1]$ .

Hence, we get  $\|P(\text{damage}|\hat{c})\|_F \in [1/\sqrt{KN}, \sqrt{K}]$ .

Finally, the result  $r_t \in [0, 1]$  can be obtained given that  $r_{\text{norm}} = 1/\sqrt{K}$  and the vector  $\text{damage}$  is normalized.

**APPENDIX B**

**PROOF OF THEOREM 2**

Firstly, we compute the final relative distance without the deceleration in advance, namely the AV not equipped with our collaborative framework. The relative distance is  $\delta_0 - v_0\tau - v_0\eta$  since the AV takes brakes with a delay of  $\tau + \eta$ .

Then for the vehicle driven by a human, its position  $d_j^p$  at time  $j$ , can be computed as follows:

$$d_j^p = d_i^p + v_0(j - i) \quad (38)$$

thus

$$d_{\text{stop}}^p = d_i^p + v_0(j - i) + \frac{1}{2} \frac{v_0^2}{|a_{\text{min}}|} \quad (39)$$

On the other hand, for the AV with our framework, it can brake earlier at time  $i + \mu + \tau + \eta$ , thus the  $v_{j+\tau+\eta}$  is:

$$v_{j+\tau+\eta} = v_0 - \sum_{t=i+\mu+\tau+\eta}^{j+\tau+\eta-1} |a_t| \quad (40)$$

Hence,  $d_{j+\tau+\eta}$  can be computed as follows:

$$\begin{aligned} &d_{j+\tau+\eta} \\ &= d_i + (\mu + \tau + \eta)v_0 - \sum_{t=i+\mu+\tau+\eta}^{j+\tau+\eta-1} \frac{v_{t+1}^2 - v_t^2}{2|a_t|} \\ &\stackrel{(a)}{\leq} d_i + (\mu + \tau + \eta)v_0 + \frac{v_0 + v_{j+\tau+\eta}}{2}(j - i - \mu) \\ &= d_i + v_0(j - i + \tau + \eta) - \frac{1}{2}|a_{\text{ave}}|(j - i - \mu)^2 \end{aligned} \quad (41)$$

where the transition (a) to deal with the distance caused by the deceleration is resulted from the assumption that the AV brakes uniformly with  $a_{\text{ave}}$  from time  $i + \mu + \tau + \eta$  to time  $j + \tau + \eta - 1$ .

Next, we compute  $d_{\text{stop}}$ :

$$\begin{aligned} &d_{\text{stop}} = d_{j+\tau+\eta} + \frac{1}{2} \frac{v_{j+\tau+\eta}^2}{|a_{\text{min}}|} \\ &= d_{j+\tau+\eta} + \frac{1}{2} \frac{v_0^2}{|a_{\text{min}}|} - \frac{v_0 \sum_{t=i+\mu+\tau+\eta}^{j+\tau+\eta-1} |a_t|}{|a_{\text{min}}|} \\ &\quad + \frac{1}{2|a_{\text{min}}|} \left( \sum_{t=i+\mu+\tau+\eta}^{j+\tau+\eta-1} |a_t| \right)^2 \\ &\stackrel{(b)}{=} d_{j+\tau+\eta} + \frac{1}{2} \frac{v_0^2}{|a_{\text{min}}|} - \frac{|a_{\text{ave}}|}{|a_{\text{min}}|} v_0(j - i - \mu) \\ &\quad + \frac{|a_{\text{ave}}|^2}{2|a_{\text{min}}|} (j - i - \mu)^2 \\ &\stackrel{(c)}{\leq} d_i + v_0(j - i + \tau + \eta) - \frac{|a_{\text{ave}}|}{|a_{\text{min}}|} v_0(j - i - \mu) \\ &\quad + \frac{1}{2} \frac{v_0^2}{|a_{\text{min}}|} - \frac{1}{2}|a_{\text{ave}}| \left[ 1 - \frac{|a_{\text{ave}}|}{|a_{\text{min}}|} \right] (j - i - \mu)^2 \end{aligned} \quad (42)$$

where (b) results from the replacement of  $\sum_{\tau=i+\mu+\tau+\eta}^{j+\tau+\eta-1} |a_{\tau}|$  to  $a_{ave}$ , and (c) comes from the inequality (41).

Hence, based on (39) and (42), we have:

$$\begin{aligned} \delta_{stop} &= d_{stop}^p - d_{stop} \\ &\geq \delta_0 - v_0\tau - v_0\eta + \frac{|a_{ave}|}{|a_{min}|} v_0(j-i-\mu) \\ &\quad + \frac{1}{2} |a_{ave}| \left[ 1 - \frac{|a_{ave}|}{|a_{min}|} \right] (j-i-\mu)^2 \end{aligned} \quad (43)$$

Finally, we get the lower bound of the relative distance  $\delta_{stop}$  in the above inequality and complete the proof.

## ACKNOWLEDGMENT

The authors would like to thank the anonymous reviewers for their valuable and constructive comments that greatly contributed to improving the quality of the paper and the editors for their support during the review process.

## REFERENCES

- [1] J. Zhang, F.-Y. Wang, K. Wang, W.-H. Lin, X. Xu, and C. Chen, "Data-driven intelligent transportation systems: A survey," *IEEE Trans. Intell. Transp. Syst.*, vol. 12, no. 4, pp. 1624–1639, Dec. 2011.
- [2] S.-H. An, B.-H. Lee, and D.-R. Shin, "A survey of intelligent transportation systems," in *Proc. IEEE 3rd Int. Conf. Comput. Intell., Commun. Syst. Netw.*, Jul. 2011, pp. 332–337.
- [3] L. Yang, R. Muresan, A. Al-Dweik, and L. J. Hadjileontiadis, "Image-based visibility estimation algorithm for intelligent transportation systems," *IEEE Access*, vol. 6, pp. 76728–76740, 2018.
- [4] H. Zhao, C. Wang, Y. Lin, F. Guillemard, S. Geronimi, and F. Aioun, "On-road vehicle trajectory collection and scene-based lane change analysis: Part I," *IEEE Trans. Intell. Transp. Syst.*, vol. 18, no. 1, pp. 192–205, Jan. 2017.
- [5] J. Levinson, J. Askeland, J. Becker, J. Dolson, D. Held, S. Kammel, J. Z. Kolter, D. Langer, O. Pink, M. Sokolsky, G. Stanek, D. Stavens, A. Teichman, M. Werling, S. Thrun, and V. Pratt, "Towards fully autonomous driving: Systems and algorithms," in *Proc. IEEE Intell. Vehicles Symp. (IV)*, Jun. 2011, pp. 163–168.
- [6] P. J. Antsaklis, K. M. Passino, and S. J. Wang, "An introduction to autonomous control systems," *IEEE Control Syst.*, vol. 11, no. 4, pp. 5–13, Jun. 1991.
- [7] D. J. Fagnant and K. Kockelman, "Preparing a nation for autonomous vehicles: Opportunities, barriers and policy recommendations," *Transp. Res. A, Policy Pract.*, vol. 77, pp. 167–181, Jul. 2015.
- [8] J. Nie, J. Zhang, W. Ding, X. Wan, X. Chen, and B. Ran, "Decentralized cooperative lane-changing decision-making for connected autonomous vehicles," *IEEE Access*, vol. 4, pp. 9413–9420, 2016.
- [9] W. Zong, C. Zhang, Z. Wang, J. Zhu, and Q. Chen, "Architecture design and implementation of an autonomous vehicle," *IEEE Access*, vol. 6, pp. 21956–21970, 2018.
- [10] M. W. Levin and S. D. Boyles, "A multiclass cell transmission model for shared human and autonomous vehicle roads," *Transp. Res. C, Emerg. Technol.*, vol. 62, pp. 103–116, Jan. 2016.
- [11] M. W. Levin and S. D. Boyles, "Effects of autonomous vehicle ownership on trip, mode, and route choice," *Transp. Res. Rec., J. Transp. Res. Board*, vol. 2493, no. 1, pp. 29–38, 2015.
- [12] J. I. Ge, S. S. Avedisov, C. R. He, W. B. Qin, M. Sadehpour, and G. Orosz, "Experimental validation of connected automated vehicle design among human-driven vehicles," *Transp. Res. C, Emerg. Technol.*, vol. 91, pp. 335–352, Jun. 2018.
- [13] S. Gong and L. Du, "Cooperative platoon control for a mixed traffic flow including human drive vehicles and connected and autonomous vehicles," *Transp. Res. B, Methodol.*, vol. 116, pp. 25–61, Oct. 2018.
- [14] X. Liu, K. Ma, and P. R. Kumar, "Towards provably safe mixed transportation systems with human-driven and automated vehicles," in *Proc. 54th IEEE Conf. Decis. Control (CDC)*, Dec. 2015, pp. 4688–4694.
- [15] S. Lefèvre, A. Carvalho, and F. Borrelli, "Autonomous car following: A learning-based approach," in *Proc. IEEE Intell. Vehicles Symp. (IV)*, Jun./Jul. 2015, pp. 920–926.
- [16] Y. Du, Y. Wang, and C.-Y. Chan, "Autonomous lane-change controller via mixed logical dynamical," in *Proc. IEEE 17th Int. Conf. Intell. Transp. Syst. (ITSC)*, Oct. 2014, pp. 1154–1159.
- [17] S. Glaser, B. Vanholme, S. Mammar, D. Gruyer, and L. Nouveliere, "Maneuver-based trajectory planning for highly autonomous vehicles on real road with traffic and driver interaction," *IEEE Trans. Intell. Transp. Syst.*, vol. 11, no. 3, pp. 589–606, Sep. 2010.
- [18] K. Dresner and P. Stone, "Sharing the road: Autonomous vehicles meet human drivers," in *Proc. IJCAI*, vol. 7, 2007, pp. 1263–1268.
- [19] T.-C. Au, S. Zhang, and P. Stone, "Semi-autonomous intersection management," in *Proc. Int. Conf. Auto. Agents Multi-Agent Syst.*, 2014, pp. 1451–1452.
- [20] A. Gupta, V. Sharma, N. K. Ruparam, S. Jain, A. Alhammad, and M. A. K. Ripon, "Context-awareness based intelligent driver behavior detection: Integrating wireless sensor networks and vehicle ad hoc networks," in *Proc. IEEE Int. Conf. Adv. Comput., Commun. Inform. (ICACCI)*, Sep. 2014, pp. 2155–2162.
- [21] J. C. Stutts, D. W. Reinfurt, L. Staplin, and E. Rodgman, "The role of driver distraction in traffic crashes," Tech. Rep., 2001.
- [22] T. A. Dingus, S. G. Klauer, V. L. Neale, A. Petersen, S. E. Lee, J. D. Sudweeks, M. A. Perez, J. Hankey, D. J. Ramsey, C. Bucher, Z. R. Doerzaph, J. Jermeland, R. R. Knipling, and S. Gupta, "The 100-car naturalistic driving study, phase ii-results of the 100-car field experiment," Nat. Highway Traffic Saf. Admin., Washington, DC, USA, Tech. Rep. HS-810 593, 2006.
- [23] W. Yan, S. Peng, C. Li, and L. Yang, "Impact to longitude velocity control of autonomous vehicle from human driver's distraction behavior," in *Proc. IEEE 86th Veh. Technol. Conf. (VTC-Fall)*, Sep. 2017, pp. 1–5.
- [24] *What's the Difference between Autonomous, Automated, Connected, and Cooperative Driving?* Accessed: Jan. 26, 2019. [Online]. Available: <https://www.andata.at/en/answer/whats-the-difference-between-autonomous-automated-connected-and-cooperative-driving.html>
- [25] B. Paden, M. Čáp, S. Z. Yong, D. Yershov, and E. Frazzoli, "A survey of motion planning and control techniques for self-driving urban vehicles," *IEEE Trans. Intell. Vehicles*, vol. 1, no. 1, pp. 33–55, Mar. 2016.
- [26] L. Baskar, B. De Schutter, J. Hellendoorn, and Z. Papp, "Traffic control and intelligent vehicle highway systems: A survey," *IET Intell. Transp. Syst.*, vol. 5, no. 1, pp. 38–52, Mar. 2011.
- [27] K. J. Åström and B. Wittenmark, *Computer-Controlled Systems: Theory and Design*. Courier Corporation, 2013.
- [28] C. G. Cassandras, D. L. Pepyne, and Y. Wardi, "Optimal control of systems with time-driven and event-driven dynamics," in *Proc. 37th IEEE Conf. Decis. Control*, vol. 1, Dec. 1998, pp. 7–12.
- [29] D. Q. Mayne, J. B. Rawlings, C. V. Rao, and P. O. M. Sokaert, "Constrained model predictive control: Stability and optimality," *Automatica*, vol. 36, no. 6, pp. 789–814, 2000.
- [30] S. Lefèvre, A. Carvalho, and F. Borrelli, "A learning-based framework for velocity control in autonomous driving," *IEEE Trans. Autom. Sci. Eng.*, vol. 13, no. 1, pp. 32–42, Jan. 2016.
- [31] Y. Gao, "Model predictive control for autonomous and semiautonomous vehicles," Ph.D. dissertation, Dept. Eng. Mech. Eng., Univ. California, Berkeley, Berkeley, CA, USA, 2014.
- [32] H. Tehrani, K. Muto, K. Yoneda, and S. Mita, "Evaluating human & computer for expressway lane changing," in *Proc. IEEE Intell. Vehicles Symp.*, Jun. 2014, pp. 382–387.
- [33] Q. H. Do, H. Tehrani, S. Mita, M. Egawa, K. Muto, and K. Yoneda, "Human drivers based active-passive model for automated lane change," *IEEE Intell. Transp. Syst. Mag.*, vol. 9, no. 1, pp. 42–56, Jan. 2017.
- [34] L. M. Bergasa, D. Almería, J. Almazán, J. J. Yebe, and R. Arroyo, "DriveSafe: An app for alerting inattentive drivers and scoring driving behaviors," in *Proc. IEEE Intell. Vehicles Symp.*, Jun. 2014, pp. 240–245.
- [35] C. Dwork, "Differential privacy: A survey of results," in *Proc. Int. Conf. Theory Appl. Models Comput.* Berlin, Germany: Springer, 2008, pp. 1–19.
- [36] C. Perfecto, J. Del Ser, M. Bennis, and M. N. Bilbao, "Beyond WYSIWYG: Sharing contextual sensing data through mmWave V2V communications," in *Proc. IEEE Eur. Conf. Netw. Commun. (EuCNC)*, Jun. 2017, pp. 1–6.
- [37] V. Va, T. Shimizu, G. Bansal, and R. W. Heath, Jr., "Millimeter wave vehicular communications: A survey," *Found. Trends Netw.*, vol. 10, no. 1, pp. 1–113, Jun. 2016.

- [38] L. Li, D. Wen, and D.Y. Yao, "A survey of traffic control with vehicular communications," *IEEE Trans. Intell. Transp. Syst.*, vol. 15, no. 1, pp. 425–432, Feb. 2014.
- [39] D. Schramm, M. Hiller, and R. Bardini, "Vehicle dynamics," in *Modeling and Simulation*. Berlin, Germany: Springer, 2014, p. 151.
- [40] J. Eggert, "Predictive risk estimation for intelligent adas functions," in *Proc. IEEE 17th Int. Conf. Intell. Transp. Syst. (ITSC)*, Oct. 2014, pp. 711–718.
- [41] S. V. Raković, E. C. Kerrigan, D. Q. Mayne, and J. Lygeros, "Reachability analysis of discrete-time systems with disturbances," *IEEE Trans. Autom. Control*, vol. 51, no. 4, pp. 546–561, Apr. 2006.
- [42] A. Carvalho, Y. Gao, S. Lefevre, and F. Borrelli, "Stochastic predictive control of autonomous vehicles in uncertain environments," in *Proc. 12th Int. Symp. Adv. Vehicle Control*, 2014, pp. 712–719.
- [43] Y. Tang, C. Peng, S. Yin, J. Qiu, H. Gao, and O. Kaynak, "Robust model predictive control under saturations and packet dropouts with application to networked flotation processes," *IEEE Trans. Autom. Sci. Eng.*, vol. 11, no. 4, pp. 1056–1064, Oct. 2014.
- [44] *State Farm Distracted Driver Detection*. Accessed: Jul. 11, 2016. [Online]. Available: <https://www.kaggle.com/c/state-farm-distracted-driver-detection/data/>
- [45] *UFLDL Tutorial*. Accessed: Jul. 19, 2016. [Online]. Available: [http://deeplearning.stanford.edu/wiki/index.php/UFLDL\\_Tutorial/](http://deeplearning.stanford.edu/wiki/index.php/UFLDL_Tutorial/)
- [46] A. Coates, A. Y. Ng, and H. Lee, "An analysis of single-layer networks in unsupervised feature learning," in *Proc. 14th Int. Conf. Artif. Intell. Statist.*, 2011, pp. 215–223.
- [47] F. Guo, S. G. Klauer, Y. Fang, J. M. Hankey, J. F. Antin, M. A. Perez, S. E. Lee, and T. A. Dingus, "The effects of age on crash risk associated with driver distraction," *Int. J. Epidemiol.*, vol. 46, no. 1, pp. 258–265, 2017.
- [48] S. G. Klauer, F. Guo, B. G. Simons-Morton, M. C. Ouimet, S. E. Lee, and T. A. Dingus, "Distracted driving and risk of road crashes among novice and experienced drivers," *New England J. Med.*, vol. 370, no. 1, pp. 54–59, 2014.
- [49] S. Kaplan, M. A. Guvensan, A. G. Yavuz, and Y. Karalurt, "Driver behavior analysis for safe driving: A survey," *IEEE Trans. Intell. Transp. Syst.*, vol. 16, no. 6, pp. 3017–3032, Dec. 2015.



tical machine learning, and autonomous vehicle control.

**WEN YAN** (S'16) received the B.S. degree in electrical engineering from Tsinghua University, Beijing, China, in 2013. He is currently pursuing the Ph.D. degree in information and communication engineering with the School of Information Science and Engineering, Southeast University, Nanjing, China. From 2017 to 2018, he was a visiting Ph.D. student with the University of Wisconsin–Madison, Madison, WI, USA. His current research interests include data mining, statistical machine learning, and autonomous vehicle control.



From July 2013 to August 2014, he was with the DSL Laboratory as a Visiting Associate Professor, supervised by Prof. J. M. Cioffi. He has been the Supervisor of Ph.D. degree students, since 2016. His research interests include in the 5G cellular transmission, underwater communications, machine learning for video signal processing, and next generation of Wi-Fi.

**CHUNGUO LI** (SM'16) received the bachelor's degree in wireless communications from Shandong University, in 2005, and the Ph.D. degree in wireless communications from Southeast University, Nanjing, in 2010.

In July 2010, he joined the Faculty of Southeast University, where he became an Associate Professor, in 2012, and a Full Professor, in 2017. From June 2012 to June 2013, he was the Postdoctoral Researcher with Concordia University, Montreal,

Dr. Li is a Senior Member of the Chinese Institute of Electronics and Chinese Computer Foundation (CCF). He is also a Fellow of IET. He was a recipient of the Best Ph.D. Thesis Award of Southeast University, in 2010, the Excellent Foreign Postdoc Award of Canada, in 2012, the Science and Technology Progress Award of the National Education Ministry of China, in 2014, the Excellent Visiting Associate Professor at Stanford, in 2014, the Southeast University Excellent Young Professor Award, in 2015, the Excellent Teaching Award of Southeast University, in 2016, the Cyrus Tang Foundation Endowed Professorship, in 2018, the Scientific Research Achievement Award of Jiangsu Province Education Department, in 2018, and several conference best paper awards. He has served for the many IEEE conferences, including the IEEE 16th International Symposium on Communications and Information Technologies as the Track Chair of Wireless Communications, Special Session Signal processing and air interface design solutions for Beyond 5G wireless communications on the IEEE PIMRC-2018 as the Chair, the International Conference on Communications, the International Conference on Acoustics, Speech and Signal Processing as a TPC Member. He is currently an Associate Editor for *IET Communications*, an Area Editor of the *AEU-International Journal of Electronics and Communications* (Elsevier), an Editor of *Telecommunications Systems*, an Associate Editor of *Circuits, Systems, and Signal Processing*, an Editor of the *KSII Transactions on Internet and Information Systems*, a Leading Guest Editor of the Special Issue Ultra-Reliable-and-Available Low-Latency Communications for 5G/B5G-enabled IoT on the *EURASIP Journal on Wireless Communications and Networking*, and a Guest Editor of the Special Issue Unmanned Aerial Vehicle Assisted Communications and Networking on *Physical Communications*. He is also a regular Reviewer for the many IEEE journals.



**YONGMING HUANG** (M'10–SM'17) received the B.S. and M.S. degrees from Nanjing University, Nanjing, China, in 2000 and 2003, respectively, and the Ph.D. degree in electrical engineering from Southeast University, Nanjing, in 2007. From 2008 to 2009, he was visiting the Signal Processing Laboratory, School of Electrical Engineering, KTH Royal Institute of Technology, Stockholm, Sweden. Since 2007, he has been a Faculty Member with the School of Information Science and Engineering, Southeast University, where he is currently a Full Professor. He has authored or coauthored more than 200 peer-reviewed articles. He holds more than 60 invention patents, and submitted more than ten technical contributions to the IEEE standards. His current research interests include multi-in multi-out wireless communications, cooperative wireless communications, and millimeter-wave wireless communications. He was elected as the Changjiang Young Scholar of Ministry of Education of China, in 2015. Since 2012, he has also been an Associate Editor of the IEEE TRANSACTIONS ON SIGNAL PROCESSING, the *EURASIP Journal on Advances in Signal Processing*, and the *EURASIP Journal on Wireless Communications and Networking*.



**LUXI YANG** (M'96–SM'17) received the M.S. and Ph.D. degree in electrical engineering from the Southeast University, Nanjing, China, in 1990 and 1993, respectively. Since 1993, he has been with the Department of Radio Engineering, Southeast University, where he is currently a Full Professor of information systems and communications, and the Director of the Digital Signal Processing Division. He has authored or coauthored two published books and more than 100 journal articles. He holds 30 patents. His current research interests include signal processing for wireless communications, MIMO communications, cooperative relaying systems, and statistical signal processing. He is currently a member of the Signal Processing Committee of Chinese Institute of Electronics. He received the first- and second-class prizes of science and technology progress awards of the state education ministry of China, in 1998, 2002, and 2014.

...